6

Vibrational and Optical Studies of Organic Conductor Nanoparticles

Dominique de Caro, Kane Jacob, Matthieu Souque and Lydie Valade
CNRS, LCC (Laboratoire de Chimie de Coordination), 205, route de Narbonne and Université de Toulouse, UPS, INPT, LCC Toulouse, France

1. Introduction

To create free electrons in organic solids and thus generate an organic material exhibiting electrical conductivity, a simple way is to build an organic complex, in which there is a charge transfer from the atoms or molecules of an electron donor (D) to those of an electron acceptor (A). In 1973, the charge transfer salt TTF·TCNQ (donor: tetrathiafulvalene, TTF; acceptor: tetracyanoquinodimethane, TCNQ) was synthesized (figure 1) (Ferraris et al., 1973). In TTF·TCNQ single crystals, TTF and TCNQ form segregated columnar stacks along the *b*-axis of the crystal structure. The interplanar spacings in the TTF and TCNQ molecular stacks at room temperature are 3.47 Å and 3.17 Å, respectively (Kistenmacher et al., 1974). The TTF and TCNQ molecular planes tilt at an angle of 24.5 ° and 34.0 °, respectively with respect to the *b*-axis forming a herringbone arrangement. As single crystals, this compound behaves like a metal (the dc conductivity increases with decreasing temperature) down to 54 K, temperature at which it undergoes a metal-to-semiconductor transition. The maximum of conductivity in TTF·TCNQ is along the *b*-axis (about 600 Ω^{-1} cm^{-1}). Conductivity values range from 10^{-2} to 1 Ω^{-1} cm^{-1} in a direction perpendicular to the direction of maximum conductivity. The amount of charge transfer from the TTF donor molecule to the TCNQ acceptor molecule has been investigated by various techniques. Using X-ray photoelectron spectroscopy, a value of 0.56 ± 0.05 has been extracted from the shape of the S2p signal (Ikemoto et al., 1977). Values in the range 0.50–0.60 have been obtained by a numerical integration of X-ray diffraction amplitudes (Coppens, 1975). However, the most convenient technique is based on infrared spectroscopy. Using the linear correlation of the nitrile stretching mode for TCNQ as a function of the degree of charge transfer, a value of 0.59 ± 0.01 has been obtained (Chappell et al., 1981).

Although synthesized for many years, TTF·TCNQ currently attracts much interest because of its interesting physical properties. Moreover, it is the one-dimensional conductor which is the most intensively processed in forms others than single crystals. For instance, TTF·TCNQ was prepared as thin films on (100)-oriented alkali halide substrates (Fraxedas et al., 2002), as self-organized monolayers on Au(111) (Yan et al., 2009), or as nanowires on stainless steel conversion coatings (Savy et al., 2007). We report in this chapter the preparation and spectral studies of TTF·TCNQ prepared as nanoparticles.

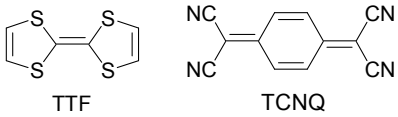

Fig. 1. Molecular structures for TTF and TCNQ

2. Nanoparticle synthesis

The TTF·TCNQ charge transfer salt is prepared by slow diffusion of an organic solution of TTF into an organic solution of TCNQ. Due to its quasi-one-dimensional character, TTF·TCNQ is commonly grown as long needles or wires. To control the growth of this material as nanospheres or nanoplatelets, a stabilizing agent is added. The stabilizing agent forms a very thin protective layer around each particle thereby preventing their aggregation. We have used ionic liquids (IL), ionic liquid/oleic acid (OA) mixtures or various other as protecting agents or stabilizing media.

Pure ionic liquids such as imidazolium salts are known to stabilize metal nanoparticles (Ru or Pd for example) exhibiting sizes lower than 10 nm (Gutel et al., 2007). The imidazolium salt alone is not suitable for the growth of TTF ·TCNQ nanoparticles because precursors are not soluble in this medium. The use of a co-solvent (*e.g.* acetonitrile or acetone, noted S) is essential. For this reason, we have performed the synthesis in a binary (IL/S) or a tertiary (IL/OA/S) mixture. The ionic liquid which has been used as a protecting species is either the 1-butyl-3-methylimidazolium tetrafluoroborate ($BMIMBF_4$, figure 2) or the 1-decyl-3-methylimidazolium tetrafluoroborate ($DMIMBF_4$). The solvent (S) is a 1:1 (vol./vol.) acetonitrile/acetone mixture.

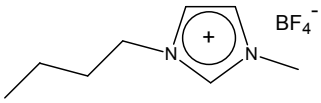

Fig. 2. Molecular structure for $BMIMBF_4$ (for $DMIMBF_4$, the butyl chain C_4H_9 is replaced by a decyl chain $C_{10}H_{21}$)

V_r	$BMIMBF_4$	$DMIMBF_4$
0.04	Nanoparticles slightly agglomerated (diameter: 2−6 nm; mean: 3.8 nm)	Mixture of spherical nanoparticles (3−18 nm), elongated nanoparticles, and nano-platelets
0.2−0.4	Well-dispersed nanoparticles (diameter: 12−62 nm; mean: 35 nm)	Well-dispersed nanoparticles (diameter: 30−100 nm; mean: 50 nm)
≥ 1	Long needles (> 5 μm long; 0.5−2 μm wide)	Long needles (> 5 μm long; 0.5−2 μm wide)

Table 1. Transmission electrons microscopy results for TTF·TCNQ prepared in the presence of an ionic liquid

The TTF precursor is solubilized in a mixture of $BMIMBF_4$ (or $DMIMBF_4$) and S whereas the TCNQ precursor is solubilized in S. The TTF solution is slowly added to the TCNQ solution

at room temperature. A fine black precipitate appears throughout the addition. The air-stable black solid, filtered off, washed and finally dried under vacuum, consists in TTF·TCNQ nanoparticles (yield ~ 50–80 %). Mean size, morphology and state of dispersion of the nanoparticles depend on the volume ratio V_r = $BMIMBF_4$/S (or $DMIMBF_4$/S), see table 1 and figures 3 and 4. The use of a tertiary mixture ($BMIMBF_4$/OA/S) in a 1:1 ratio (vol./vol.) $BMIMBF_4$/OA leads to clusters of nanoparticles (cluster size: 150–400 nm, size of individual particles in a cluster: 8–25 nm). For a 1:3 ratio (vol./vol.) $BMIMBF_4$/OA, well dispersed nanoparticles exhibiting a mean diameter of 40 nm are obtained.

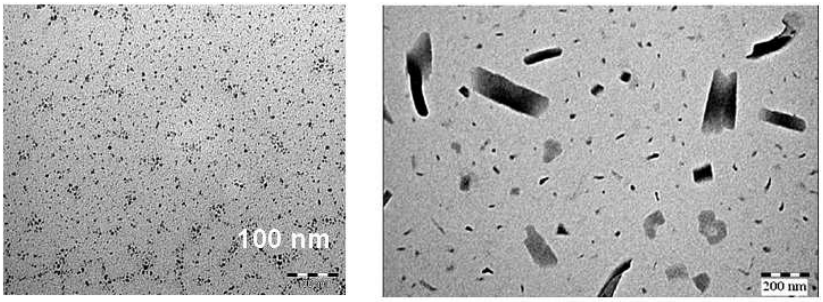

Fig. 3. Electron micrographs for TTF·TCNQ in the presence of $BMIMBF_4$ (left, V_r = 0.04) and $DMIMBF_4$ (right, V_r = 0.04)

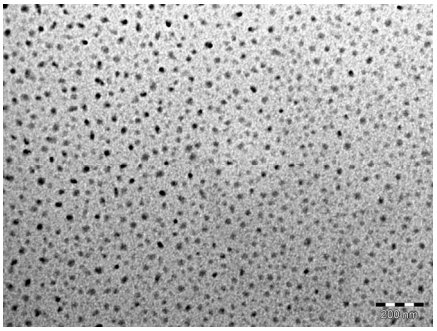

Fig. 4. Electron micrograph for TTF·TCNQ in the presence of $BMIMBF_4$ (V_r = 0.4); bar = 200 nm

3. Optical properties of TTF·TCNQ nanoparticles

The electronic properties of one-dimensional systems are governed by three types of interactions among the unpaired electrons occupying the highest molecular orbital in the solid. These interactions are (i) the overlap of the wave functions of these electrons between adjacent sites in the crystal, (ii) the interactions of the electrons with their surroundings (*e.g.* phonons), and (iii) the Coulomb interaction between electrons. Theoretical models taking into account interactions (i) are usually based on a tight-binding method for the band structure. The energy bands are of the form:

$$E(k) = \pm 2t \cos(k a) + \text{const.} \quad (1)$$

where k is the wave vector, a the lattice constant, and t is the transfer matrix element between sites, given by:

$$t = \left\langle \phi_i \middle| H \middle| \phi_{i+1} \right\rangle \tag{2}$$

where H is the total Hamiltonian of the systems, and ϕ_i is the appropriate molecular orbital wave function.

The width of the band, w = 4t, depends upon the overlap of electronic wave functions, and a one-dimensional character for the bands is obtained by allowing this overlap to occur only in one direction. For partially filled bands, the system will be a metal, with a complex dielectric function:

$$\varepsilon(\omega) = \varepsilon_\infty - \frac{\omega_p^2}{\omega^2 + i\frac{\omega}{\tau}} \tag{3}$$

where ε_∞ is the dielectric constant at high frequency arising from core polarisability, τ is the electron relaxation time and ω_p is the plasma frequency. For typical one-dimensional charge-transfer based organic conductors, it has been found that $\varepsilon_\infty \sim 3$, $\tau \sim 10^{-15}$ s, and $\omega_p \sim 10000$ cm^{-1}. Several peaks (undoubtedly characterizing a charge-transfer-based organic conductor) can be seen on electronic spectra recorded either in solution or in the solid state. In addition to the plasma frequency, four absorption bands are usually observed: the first one is at $(2–4)\times10^3$ cm^{-1}, the second at about $(10–12)\times10^3$ cm^{-1}, the third one at about $(16–18)\times10^3$ cm^{-1}, and the fourth one at about $(25–31)\times10^3$ cm^{-1}. The first one is assigned to the charge transfer of the type $A^-A^0 \rightarrow A^0A^-$, where A^- and A^0 denote the anion and the neutral molecule of the electron acceptor, respectively (CT1 band). The second one is attributed to the charge transition of the type $A^-A^- \rightarrow A^0A^{2-}$ (CT2 band). The third one is the local excitation associated with the lowest intramolecular transition of A^- (LE1 band), whereas the fourth one is due to the local excitation associated with the lowest intramolecular transition of A^0 (LE2 band).

The room temperature reflectance spectrum of a nanoparticle film of TTF·TCNQ has been recorded in the 9000–25000 cm^{-1} range (figure 5). The general shape of this spectrum is in good agreement with that of TTF·TCNQ single crystals, recorded for an electric field polarized parallel to the *b* crystallographic axis (Grant et al., 1973). The plasma reflection is clearly seen at 10700 cm^{-1} (about 1.32 eV), in excellent agreement with that obtained for TTF ·TCNQ single crystals (1.38 eV) (Grant et al., 1973). The conduction-band width (w = 4t) can be estimated from the measured plasma frequency, using the expression:

$$w = \frac{h^2\,\omega_p^2}{16\,\pi^2\,N\,e^2\,b} \tag{4}$$

where N denotes the electron density and *b* the lattice parameter (3.819 Å). Taking the value of 4.7×10^{21} cm^{-3} for N (Bright et al., 1974), we find w = 0.59 eV, in good agreement with the w value calculated for TTF·TCNQ single crystals (0.62 eV) (Graja, 1997). It is to be noticed that the X-ray diffraction pattern of the nanoparticle film is dominated by the (002), (004), and (008) lines. This indicates a preferential orientation of the film, *i.e.* the *ab* plane being parallel to the substrate surface. In our case, the light is unpolarized and interacts with the

substrate surface according to all possible angles (integrating sphere). However, our reflectance spectrum is as good as that recorded for a light polarized parallel to the *b* axis.

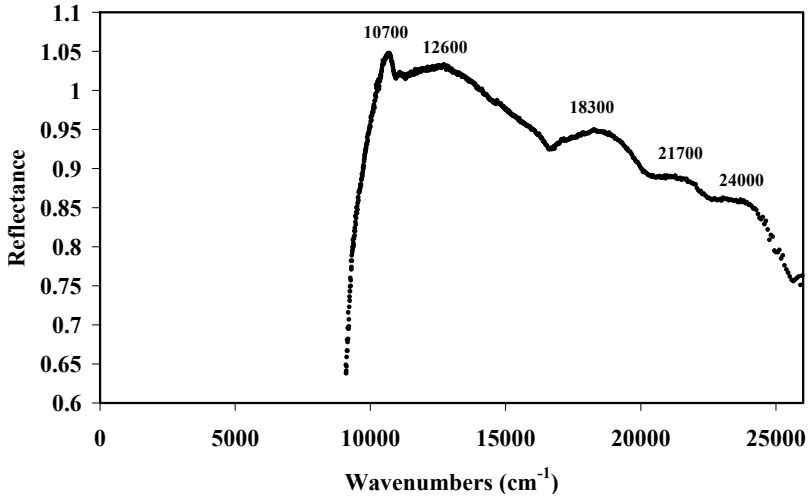

Fig. 5. Reflectance spectrum for a nanoparticle film of TTF·TCNQ (mean diameter of individual particles: 35 nm)

Furthermore, four broads signals are observed at 12600 (CT2), 18300 (LE1), 21700, and 24000 (LE2) cm^{-1} (figure 5). These four signals are also observed in the reflectance spectrum of TTF·TCNQ single crystals (12000, 17000, 22000, and 25800 cm^{-1}) (Grant et al., 1973). The absorption spectrum of TTF·TCNQ nanoparticles dispersed in acetonitrile (figure 6) also clearly evidences CT2, LE1, and LE2 bands at 11900, 16400–19000, and 26000 cm^{-1}, respectively

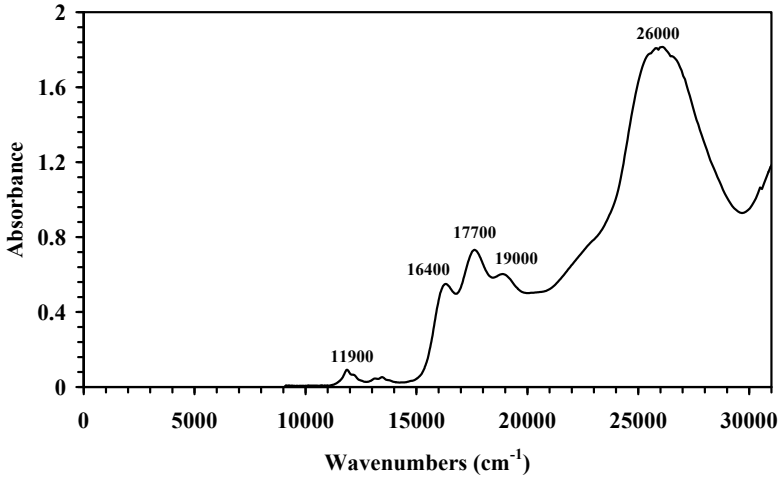

Fig. 6. Absorption spectrum for TTF·TCNQ nanoparticles dispersed in acetonitrile solution (mean diameter: 35 nm)

4. Vibrational properties of TTF·TCNQ nanoparticles

Vibrational spectroscopy (infrared and Raman) is a powerful tool to investigate one-dimensional organic charge-transfer complexes. At large distances between the donor (D) and the acceptor (A) molecules, the vibrational spectrum of D + A is just the sum of those of the free molecules. As the distance between them becomes shorter (formation of the D−A complex), the electrostatic field of one molecule begins to influence the second one, and vice-versa. This causes changes in the frequency and intensity from the spectra of isolated molecules. Moreover, due to the fact that the D (or A) molecule may have a lower symmetry in D−A, additional frequencies appear in the complex because forbidden modes may become active due to mixing with other internal modes of D (or A). The vibrational spectrum consists of a primary electronic charge transfer band (CT1) and a series of oscillations driven by totally symmetric internal molecular vibrations (a_g modes) of one or both parts of the complex.
In the infrared spectrum of ionic liquid-stabilized TTF·TCNQ nanoparticles, vibration bands for $BMIMBF_4$ or $DMIMBF_4$ are not observed. However, its presence and thus its stabilizing role have been evidenced by X-ray photoelectron spectroscopy. Indeed, the X-ray photoelectron spectrum shows boron and fluorine lines which can only be due to the ionic liquid. Moreover, the $S2p_{3/2}$ signal (163.6 eV) is in excellent agreement with that previously reported for TTF·TCNQ single crystals, *i.e.* 163.8 eV (Butler et al., 1974). In the spectrum of ionic liquid/oleic acid (OA)-stabilized TTF·TCNQ nanoparticles, vibration bands for OA are present, thus confirming that oleic acid forms a protecting layer around the nanoparticles. However, this stabilizing role is effective when oleic acid is at least introduced in a volume three times higher than that of the ionic liquid. Whatever the stabilizing agent, the infrared spectrum of nanoparticles recorded at room temperature in a KBr matrix (figure 7) is quite similar to that previously described for TTF·TCNQ processed as thin films (Wozniak et al., 1975; Benoit et al., 1976). Moreover, the infrared spectrum is weakly particle size-dependent. Peak positions and assignments are given in table 2.

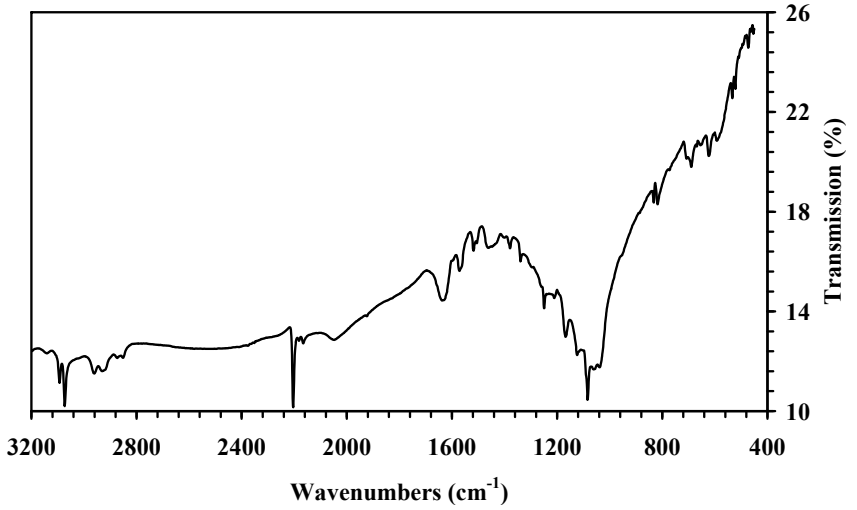

Fig. 7. Infrared spectrum at 298 K for TTF·TCNQ nanoparticles dispersed in KBr matrix (mean diameter: 35 nm; stabilizing agent: $BMIMBF_4$)

Assignment	νCH	νCH	νCN	νCN	νC=C	νC=C	–	–	δS–C–H	νC–S
1	3093	3073	2204	2182	1571	1518	1340	1170	1083	832/ 817
2	–	–	2207	2190	1552	1537	1355	1182	1096	797/ 786
3	–	–	very broad	–	1580	–	–	–	1080	798

Table 2. Infrared modes (cm^{-1}) and assignments for TTF·TCNQ nanoparticles (mean diameter: 35 nm; stabilizing agent: $BMIMBF_4$) and thin films. 1: our work; 2: Wozniak et al., 1975; 3: Benoit et al., 1976

Our spectrum clearly evidences C(sp^2)−H at 3093 and 3073 cm^{-1}. These modes are surprisingly not observed for TTF·TCNQ thin films deposited on NaCl or KBr crystals (Wozniak et al., 1975; Benoit et al., 1976). In our case, the characteristic nitrile doublet is located at 2204 and 2182 cm^{-1}. The more intense signal at 2204 cm^{-1} allows us to determine the amount of charge transfer from the TTF donor molecule to the TCNQ acceptor molecule. Using the linear correlation of the nitrile stretching mode for TCNQ as a function of the degree of charge transfer, we obtain a value of 0.56, in relatively good agreement with that for single crystals, *i.e.*, 0.59 (Chappell et al., 1981). Thus, the charge transfer in an assembly of nanoparticles is rather similar to that on a macroscopic single crystal. The position, the intensity and the width at half maximum for carbon-carbon double bond modes (in the 1500−1600 cm^{-1} range) are usually sample preparation and temperature dependent. For TTF·TCNQ nanoparticles, they are located at 1571 and 1518 cm^{-1}. Finally, the characteristic doublet for TTF (C−S stretch) is located at 832/817 cm^{-1} for us and at 797/786 cm^{-1} for TTF·TCNQ thin films. This large difference (about 30 cm^{-1}) can be an effect of the temperature (spectra recorded at room temperature in our case and at 10 K for TTF·TCNQ thin films, see Wozniak et al., 1975).

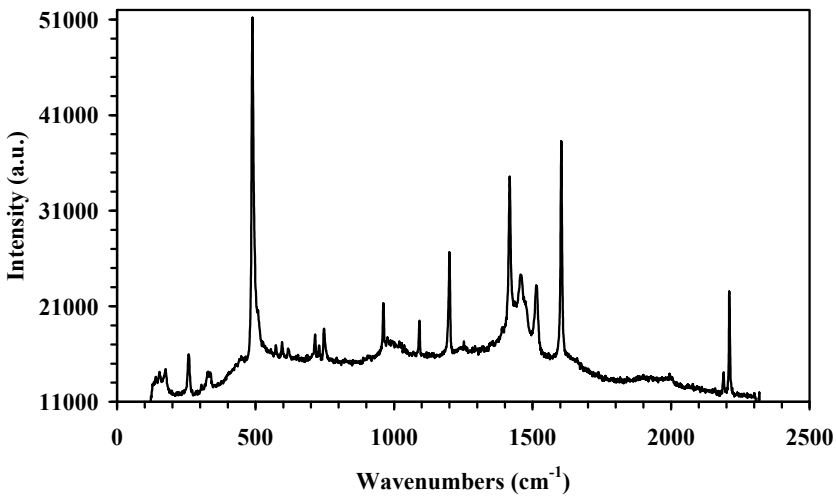

Fig. 8. Raman spectrum at 77 K for TTF·TCNQ as a nanoparticle film (mean diameter of individual particles: 35 nm; stabilizing agent: $BMIMBF_4$)

Raman spectroscopy is widely used to study the vibrational and structural properties of molecule-based conductors as single crystals. This form is the best suited for obtaining the best signal to noise ratio. However, this technique is also well suited for studying thin molecular layers (oriented, Langmuir-Blodgett, nanoparticle, or polymer films). The TTF·TCNQ nanoparticles are dispersed in diethyl ether and deposited on a glass slide. The solvent is then evaporated slowly. Raman spectra are obtained at 77 K using the 647 nm line of a Kr laser (power ~ 1.7×10^6 W cm^{-2}). The incident beam is focused onto the film through the ×100 microscope objective, giving a spot size of ~ 1 μm^2. The back-scattered light is collected through the same objective, dispersed and then imaged onto a CCD detector. Whatever the ionic liquid used as stabilizing agent, the Raman spectrum of the nanoparticle film (figure 8) is quite similar to that previously described for TTF·TCNQ single crystals

ν (cm^{-1})	Assignment	Symmetry
260 (263)	–	–
339 (333)	Ring deformation in TCNQ	a_g (ν_9)
489 (502)	C−S stretch and C−S−C bend	b_{3g} (ν_{47})
573 (572)	–	b_{2g} (ν_{29})
596 (600)	$C(CN)_2$ scissor	a_g (ν_8)
716 (714)	C−C ring stretch	a_g (ν_7)
748 (755)	C−S stretch	b_{2g} (ν_{28})
962 (962)	C−C ring stretch	a_g (ν_6)
1200 (1202)	C−C−H bend and C=C ring stretch in TCNQ	a_g (ν_5)
1418 (1423)	C=C stretch in TCNQ	a_g (ν_4)
1461 (1456)	C=C stretch centre and C=C stretch ring in TTF	–
1516 (1520)	C=C stretch centre and C=C stretch ring in TTF	a_g (ν_3)
1604 (1606)	C=C ring stretch in TCNQ	–
2210 (2224)	C≡N stretch	a_g (ν_2)

Table 3. Raman modes, assignments, and symmetry for TTF·TCNQ as a nanoparticle film (mean diameter of individual particles: 35 nm; stabilizing agent: $BMIMBF_4$) and as single crystals. In parentheses: values from Graja, 1997 or Kuzmany & Stolz, 1977

(Kuzmany & Stolz, 1977). An assignment of nearly all of the peaks can be found by comparing our results with the latter. In table 3, we compile the most important lines, their assignment, and their symmetry.

Except the nitrile stretching mode, all peak positions for TTF·TCNQ nanoparticles are very similar to those on single crystals (see values in parentheses on table 3). The C≡N stretching mode for TTF·TCNQ nanoparticles is located at 2210 cm^{-1} in the Raman spectrum whereas it is located at 2204 cm^{-1} in the infrared spectrum (figure 7 and table 2). This difference is still relatively low given the uncertainties on the positions of signals (± 4 cm^{-1}) for both spectral techniques. The following discussion will be mainly based on the totally symmetric a_g modes. These modes (10 for the TCNQ molecule and 7 for the TTF molecule) have been intensively studied for neutral (TTF^0, $TCNQ^0$), anionic ($TCNQ^-$), or cationic (TTF^+) species (Graja, 1997). The conduction electrons in TTF·TCNQ are significantly coupled to almost all intramolecular vibration (a_g) modes. The more significant ones (from ν_2 to ν_6) have been used to investigate the charge transfer in TTF·TCNQ single crystals (Kuzmany & Stolz, 1977). Table 4 gathers a_g ν_2 to ν_6 modes (column two) for TTF·TCNQ nanoparticles, for neutral TCNQ (column three) and for the $TCNQ^-$ anion (column four). Comparing column two with columns three and four in table 4, evidences that the Raman lines of TTF·TCNQ are generally within the limits of neutral and completely charged TCNQ.

	TTF·TCNQ nanoparticles	$TCNQ^0$	$TCNQ^-$	ρ
ν_2	2210	2230	2192	−0.53
ν_3	1604	1602	1613	−0.18
ν_4	1418	1453	1389	−0.55
ν_5	1200	1207	1195	−0.58
ν_6	962	932	960	−1.07

Table 4. A_g modes (in cm^{-1}) for TTF·TCNQ nanoparticles, neutral TCNQ and radical anion, and evaluation of the charge transfer in TTF·TCNQ as nanoparticles

According to Graja, the charge (ρ) borne by the TCNQ molecule can be calculated as follows:

$$\rho = \frac{\nu - \nu_0}{\nu_0 - \nu_{-1}} \tag{5}$$

where ν is the vibrational frequency for TTF·TCNQ, ν_0 the vibrational frequency for neutral TCNQ, and ν_{-1} the vibrational frequency for $TCNQ^-$. Values of ρ obtained from equation (5) are given in table 4. Kuzmany & Stolz admit that the negative charge borne by the TCNQ molecule in TTF·TCNQ is the average of all charges as compiled in table 4 (column five). In

our case, the average charge is found to be –0.58, in excellent agreement with that for single crystals, *i.e.*, –0.59 (Chappell et al., 1981).

5. Conclusion

In this chapter, we have shown that the famous organic charge transfer-based conductor TTF·TCNQ can be processed as roughly spherical nanoparticles, while this compound has a natural tendency to grow as needles. The growth as nanospheres is controlled by the use of an ionic liquid introduced together with a conventional solvent. Under certain conditions, well dispersed nanoparticles exhibiting sizes lower than 50 nm can be obtained. Optical and vibrational studies have been performed on either TTF·TCNQ dispersed in an infrared transparent matrix, or on a nanoparticle film, or dispersed in solution. Optical and vibrational signatures for TTF·TCNQ as nanoparticles are in good agreement with those on single crystals, on powders exhibiting micrometer-sized grains, or on thin films. We do expect transport properties similar as the two latter. Preliminary conductivity measurements on a nanoparticle film (mean diameter of individual nanoparticles: 4 nm or 35 nm) have been performed using the four probe technique. TTF·TCNQ nanoparticle films exhibit a semiconducting behavior, which is not surprising for nanopowdered materials (room-temperature conductivity: 10−20 S cm^{-1}, activation energy: 15−40 meV). We are currently working on the use of dielectric spectroscopy to characterize an assembly of TTF·TCNQ nanoparticles. We are also developing the use of Raman spectroscopy (at low temperatures) to investigate the charge transfer in nanoparicles of organic or metallo-organic superconducting phases.

6. Acknowledgment

The authors appreciate the contribution and collaboration of the following persons: C. Faulmann (LCC−Toulouse, France); H. Hahioui (University of Rabat, Morocco); C. Routaboul (LCC−Toulouse and University Paul Sabatier, France); F. Courtade and J.-M. Desmarres (CNES−Toulouse, France); O. Vendier (Thales Alenia Space−Toulouse, France); J. Fraxedas (CIN2−Barcelona, Spain).

7. References

The order of reference is that of citation in the text.

Ferraris, J.; Cowan, D. O.; Walatka, Jr., V. & Perlstein, J. H. (1973). Electron transfer in a new highly conducting Donor−Acceptor complex. *Journal of the American Chemical Society,* Vol. 95, No. 3, (February 1973), pp. 948-949.

Kistenmacher, T. J.; Phillips, T. E. & Cowan D. O. (1974). The crystal structure of the 1:1 radical cation−radical anion salt of 2,2′-bis-1,3-dithiole (TTF) and 7,7,8,8-tetracyanoquinodimethane (TCNQ). *Acta Crystallographica B,* Vol. 30, No. 3, (March 1974), pp. 763-768.

Ikemoto, I.; Sugano, T. & Kuroda H. (1977). Evaluation of the charge transfer in tetrathiofulvalene-tetracyanoquinodimethane (TTF-TCNQ) and related complexes

from X-ray photoelectron spectroscopy. *Chemical Physics Letters,* Vol. 49, No. 1, (July 1977), pp. 45-48.

Coppens, P. (1975). Direct evaluation of the charge transfer in tetrathiafulvalene-tetracyanoquinodimethane (TTF-TCNQ) complex at 100 K by numerical integration of X-ray diffraction amplitudes. *Physical Review Letters,* Vol. 35, No. 2, (July 1975), pp. 98-100.

Chappell, J. S.; Bloch, A. N.; Bryden, W. A.; Maxfield, M.; Poehler, T. O. & Cowan, D. O. (1981). Degree of charge transfer in organic conductors by infrared absorption spectroscopy. *Journal of the American Chemical Society,* Vol. 103, No. 9, (May 1981), pp. 2442-2443.

Fraxedas, J.; Molas, S.; Figueras, A.; Jiménez, I.; Gago, R.; Auban-Senzier, P. & Goffman, M. (2002). Thin films of molecular metals: TTF-TCNQ. *Journal of Solid State Chemistry,* Vol. 168, No. 2, (November 2002), pp. 384-389.

Yan, H.; Li, S.; Yan, C.; Chen, Q. & Wan, L. (2009). Absorption of TTF, TCNQ and TTF-TCNQ on Au(111): An *in situ* ECSTM study. *Science in China Series B: Chemistry,* Vol. 52, No. 5, (May 2009), pp. 559-565.

Savy, J.-P.; de Caro, D.; Faulmann, C.; Valade, L.; Almeida, M.; Koike, T.; Fujiwara, H.; Sugimoto, T.; Fraxedas, J.; Ondarçuhu, T. & Pasquier, C. (2007). Nanowires of molecule-based charge-transfer salts. *New Journal of Chemistry,* Vol. 31, No. 4, (April 2007), pp. 519-527.

Gutel, T.; Garcia-Antõn, J.; Pelzer, K.; Philippot, K.; Santini, C. C.; Chauvin, Y.; Chaudret, B. & Basset, J. M. (2007). Influence of the self-organization of ionic liquids on the size of ruthenium nanoparticles: effect of the temperature and stirring. *Journal of Materials Chemistry,* Vol. 17, No. 31, (August 2007), pp. 3290-3292.

Grant, P. M.; Greene, R. L.; Wrighton, G. C. & Castro, G. (1973). Temperature dependence of the near-infrared optical properties of tetrathiofulvalinium-tetracyanoquinodimethane (TTF-TCNQ). *Physical Review Letters,* Vol. 31, No. 21, (November 1973), pp. 1311-1314.

Bright, A. A.; Garito, A. F. & Heeger, A. J. (1974). Optical conductivity studies in a one-dimensional organic metal: tetrathiofulvalene tetracyanoquinodimethane (TTF)(TCNQ). *Physical Review B,* Vol. 10, No. 4, (August 1974), pp. 1328-1342.

Graja, A. (1997). *Spectroscopy of materials for molecular electronics* (first edition), Scientific Publishers OWN and Polish Academy of Sciences, 83-85481-23-0, Poznań

Butler, M. A.; Ferraris, J. P.; Bloch, A. N. & Cowan, D. O. (1974). Electron transfer in TTF-TCNQ and related compounds. *Chemical Physics Letters,* Vol. 24, No. 4, (February 1974), pp. 600-602.

Wozniak, W. T.; Depasquali, G.; Klein, M. V.; Sweany, R. L. & Brown, T. L. (1975). Vibrational spectra of TTF-TCNQ: evidence of TTF^0 and $TCNQ^0$ in thin films. *Chemical Physics Letters,* Vol. 33, No. 1, (May 1975), pp. 33-36.

Benoit, C.; Galtier, M.; Montaner, A.; Deumie, J.; Robert, H. & Fabre, J.-M. (1976). Temperature dependence of infrared spectra of TTF(TCNQ) thin films. *Solid State Communications,* Vol. 20, No. 3, (October 1976), pp. 257-259.

Kuzmany, H. & Stolz, H. J. (1977). Raman scattering of TTF-TCNQ and related compounds. *Journal of Physics C: Solid State Physics,* Vol. 10, No. 12, (June 1977), pp. 2241-2252.

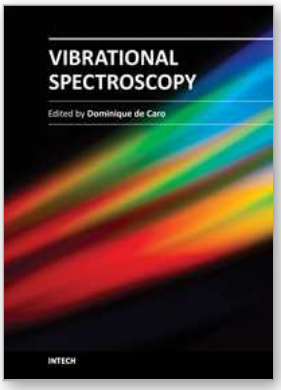

Vibrational Spectroscopy

Edited by Prof. Dominique De Caro

ISBN 978-953-51-0107-9
Hard cover, 168 pages
Publisher InTech
Published online 24, February, 2012
Published in print edition February, 2012

The infrared and Raman spectroscopy have applications in numerous fields, namely chemistry, physics, astronomy, biology, medicine, geology, mineralogy etc. This book provides some examples of the use of vibrational spectroscopy in supramolecular chemistry, inorganic chemistry, solid state physics, but also in the fields of molecule-based materials or organic-inorganic interfaces.

How to reference

In order to correctly reference this scholarly work, feel free to copy and paste the following:

Dominique de Caro, Kane Jacob, Matthieu Souque and Lydie Valade (2012). Vibrational and Optical Studies of Organic Conductor Nanoparticles, Vibrational Spectroscopy, Prof. Dominique De Caro (Ed.), ISBN: 978-953-51-0107-9, InTech, Available from: http://www.intechopen.com/books/vibrational-spectroscopy/vibrational-and-optical-studies-of-organic-conductor-nanoparticles

INTECH
open science | open minds

InTech Europe
University Campus STeP Ri
Slavka Krautzeka 83/A
51000 Rijeka, Croatia
Phone: +385 (51) 770 447
Fax: +385 (51) 686 166
www.intechopen.com

InTech China
Unit 405, Office Block, Hotel Equatorial Shanghai
No.65, Yan An Road (West), Shanghai, 200040, China
中国上海市延安西路65号上海国际贵都大饭店办公楼405单元
Phone: +86-21-62489820
Fax: +86-21-62489821

© 2012 The Author(s). Licensee IntechOpen. This is an open access article distributed under the terms of the Creative Commons Attribution 3.0 License, which permits unrestricted use, distribution, and reproduction in any medium, provided the original work is properly cited.